Crystal and Electronic Structures of Radical Salts of 2,7-Bis(methylthio)-1,6-dithiapyrene (MTDTPY) and 2,7-Bis(methylseleno)-1,6-dithiapyrene (MSDTPY)

Atsushi KAWAMOTO, Jiro TANAKA,* Akio ODA,† Hideshi MIZUMURA,†
Ichiro MURATA,† and Kazuhiro NAKASUJI††
Department of Chemistry, Faculty of Science, Nagoya University, Chikusa-ku,Nagoya 464
†Department of Chemistry, Faculty of Science, Osaka University, Toyonaka, Osaka 560
††Institute for Molecular Science, Myodaiji, Okazaki 444
(Received December 18, 1989)

Radical salts of 2,7-bis(methylthio)-1,6-dithiapyrene (MTDTPY) with PF_6^- and 2,7-bis(methylseleno)-1,6-dithiapyrene (MSDTPY) with AsF_6^- and $[Au(CN)_2]^-$ were prepared using an electrochemical method. The crystal structures of these salts were determined with an X-ray method. MTDTPY-$(PF_6)_{0.67}$ (triclinic $P\bar{1}$) and MSDTPY-$(AsF_6)_{0.67}$ (triclinic $P\bar{1}$) form uniform segregated stacks of MTDTPY and MSDTPY molecules with interplanar distances of 3.40 and 3.59 Å, respectively. Short S-S contacts of 3.46—3.56 Å for MTDTPY-$(PF_6)_{0.67}$ and 3.54—3.61 Å for MSDTPY-$(AsF_6)_{0.67}$ were observed between the columns. The chains of disordered PF_6^- and AsF_6^- were found to be parallel to the stack axis. Analysis of the disorder showed a stoichiometric ratio of the DTPY derivatives and counter anions at 1 : 0.67; the formal charge of MTDTPY and MSDTPY was estimated at +0.67. MSDTPY-$Au(CN)_2$ (monoclinic P2/c) forms a segregated stack of MSDTPY molecules with an interplanar distance of 3.40 Å. The optical reflection spectra of these crystals were measured with polarized light both parallel and perpendicular to the stack axis. In spite of the short intercolumnar S-S contacts, the spectra of MTDTPY-$(PF_6)_{0.67}$ and MSDTPY-$(AsF_6)_{0.67}$ showed a strong one-dimensional character. The optical conductivity spectra ($\sigma(\omega)$) and the real part of the dielectric constant ($\varepsilon'(\omega)$) along the stack axis were obtained by means of Kramers-Kronig transformation. Both the conductivity spectra and the dielectric constant substantially differ from the simple Drude model. These results were analyzed with a one-dimensional electron-localization model in a disordered system with the following optical parameters: ω_p=14000 cm^{-1}; τ_i=2.2×10^{-15}s (τ_i^{-1}=2400 cm^{-1}) and ε_{core}=3.0 for MTDTPY-$(PF_6)_{0.67}$ and ω_p=10000 cm^{-1}; τ_i=2.2×10^{-15}s (τ_i^{-1}=2400 cm^{-1}) and ε_{core}=3.5 for MSDTPY-$(AsF_6)_{0.67}$. From the spectra of MSDTPY-$Au(CN)_2$, the on-site Coulomb repulsion U was estimated at 6000 cm^{-1}.

In the field of synthetic organic metals, tetrathiafulvalene (TTF) and its derivatives have been widely investigated.[1] Some of the tetramethyltetraselenafulvalene (TMTSF) radical salts[2] and bis(ethylenedithio)-tetrathiafulvalene (BEDT-TTF) radical salts[3] have shown superconductivity. It is thus important to design new components for organic metals in order to find the mechanism of metallic conductivity and superconductivity. Nakasuji et al. designed new donors, (3,10-dithiaperylene (DTPR) and 1,6-dithiapyrene DTPY)) which belong to a class of peri-fused Weitz-type donors.[4] These new donors are substituted with either methylthio or methylseleno groups in order to increase the dimensionality of the conducting chains. Actually, in charge-transfer complexes of 2,7-bismethylthio)-1,6-dithiapyrene (MTDTPY) (Fig. 1) with TCNQ and chloranil, short S-S contacts are found and metallic conductivity was observed.[5]

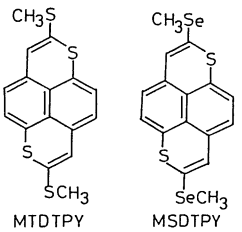

Fig. 1. Molecular structures of MTDTPY and MSDTPY.

In this paper we present structural studies concerning the radical salts of MTDTPY with PF_6^- and 2,7-bis(methylseleno)-1,6-dithiapyrene (MSDTPY) (Fig. 1), with AsF_6^- and $[Au(CN)_2]^-$ prepared by an electrochemical method. We determined the crystal structures of these salts with an X-ray method and measured the polarized reflection spectra (200—20000 cm^{-1}) along directions both parallel and perpendicular to the stack axis. Based on a one-dimensional electron localization model, we could explain the infrared spectra which characterize the behavior of conducting electron.

Experimental

Preparation of Single Crystals of MTDTPY-$(PF_6)_{0.67}$: Single crystals of 2,7-MTDTPY-$(PF_6)_{0.67}$ suitable for X-ray crystal structure analysis and reflection-spectra measurements were grown using electrocrystallization techniques. A solution of 2,7-MTDTPY (0.1 M, 1 M=1 mol dm^{-3}) in acetonitrile containing n-Bu_4NPF_6 (0.6 M) was oxidized on a platinum anode at a constant current (1.0 μA) for several days. The resulting black plates were collected and dried. The stoichiometry was deduced from a structural analysis.

Preparation of 2,7-Bis(methylseleno)-1,6-dithiapyrene (MSDTPY): To a solution of 1,6-dithiapyrene (960 mg, 4.00 mmol) in tetrahydrofuran (200 mL) was added 1.5 M n-BuLi (16.0 mL, 24 mmol) in hexane at −70 °C. After 30 min. stirring, selenium powder (156 g (20.0 mmol)) was added. The resulting mixture was allowed to warm to 0 °C

over 1 h and was then cooled to −70 °C. To the mixture was added methyl iodide (1.56 mL, 25 mmol); this mixture was allowed to warm to room temperature. After evaporation of the tetrahydrofurane, the mixture was treated with water and extracted with dichloromethane. The extracts were dried over magnesium sulfate and concentrated under reduced pressure. Recrystallization from benzene gave 2,7-bis(methylseleno)-1,6-dithiapyrene (MSDTPY) (1.26 g, 74%): Orange plates, mp 185 °C; ^{1}H NMR δ=2.24 (6H, s), 6.07 (2H, d, J=8.0 Hz), 6.10 (2H, s), 6.23 (2H, d, J=8.0 Hz); UV λ_{max} (toluene) 292 nm (sh log ε 4.05), 434 (3.99), 456 (4.04); MS m/z (relative intensity) 428 (M^+, 100%); Anal. Calcd for $C_{16}H_{12}S_2Se_2$: C, 45.08; H, 2.84%. Found: C, 45.27; H, 2.84%.

Preparation of Single Crystals of MSDTPY Salts: Single crystals of MSDTPY-$(AsF_6)_{0.67}$ and MSDTPY-$Au(CN)_2$ were grown using electrocrystallization techniques. A solution of MSDTPY (0.1 M) in dichloromethane containing n-Bu_4NAsF_6/n-$Bu_4N[Au(CN)_2]$ (0.6 M) was oxidized on a platinum anode at a constant current (3.5 μA) for several days. The resulting black needles were collected and dried. The stoichiometry was determined by elemental analysis. MSDTPY-$(AsF_6)_{0.67}$: Calcd for $C_{16}H_{12}S_2Se_2(AsF_6)_{0.67}$: C, 34.76; H, 2.19%. Found: C, 34.86; H, 2.38%. MSDTPY-$Au(CN)_2$: Calcd for $C_{16}H_{12}S_2Se_2Au(CN)_2$: C, 32.01; H, 1.79%. Found: C, 32.20; H, 1.87%.

X-ray Study: X-ray diffraction data were collected using a Rigaku automated four-circle diffractometer with Mo$K\alpha$ radiation (λ=0.7093 Å) monochromatized by graphite. The $2\theta-\omega$ scan mode was employed ($2\theta_{max}$=50°). MTDTPY-$(PF_6)_{0.67}$ and MSDTPY-$(AsF_6)_{0.67}$ showed diffuse scattering in addition to normal Bragg reflections in the oscillation photographs on the planes perpendicular to the c-axis. The diffuse layers were indexed on the basis of a superstructure spacing of 6.45 Å and 6.57 Å for MTDTPY-$(PF_6)_{0.67}$ and MSDTPY-$(AsF_6)_{0.67}$, respectively. Three standard reflections, which were measured every 100 reflections, decay less than 1, 1 and 3% for MSDTPY-$(AsF_6)_{0.67}$, MSDTPY-$(AsF_6)_{0.67}$, and MSDTPY-$Au(CN)_2$, respectively. The experimental details and crystal data are given in Table 1.

The structures were solved by a Monte-Carlo direct method[6] with the aid of the MULTAN-78 program system.[7] It was refined using a full-matrix least-square method on F[2 8] with anisotropic temperature factors. In MSDTPY-$(AsF_6)_{0.67}$, no H atoms were allocated; in MSDTPY-$(AsF_6)_{0.67}$ and MSDTPY-$Au(CN)_2$, all H atoms were allocated from a differential Fourier map and were refined with isotropic temperature factors equivalent to the bonded carbon atoms. Atomic scattering factors were taken from *International Tables for X-ray Crystallography*.[9] Finally, we obtained values for R ($R=\sum||F_o|-|F_c||/\sum|F_o|$) and R_w ($R_w=\sum w||F_o|-|F_c||/\sum w|F_o|$) of 0.083 and 0.079 for MTDTPY-$(PF_6)_{0.67}$, 0.116 and 0.098 for MSDTPY-$(AsF_6)_{0.67}$ and 0.042 and 0.039 for MSDTPY-$Au(CN)_2$, respectively. All calculations were carried out on FACOM M780 and FACOM VP200 computers at the Nagoya University Computer Center. The final positional parameters and equivalent isotropic thermal parameters of MTDTPY-$(PF_6)_{0.67}$, MSDTPY-$(AsF_6)_{0.67}$ and MSDTPT-$Au(CN)_2$ are given in Tables 2, 3 and 4, respectively. The complete F_o-F_c tables, atomic parameters of the H atoms and the anisotropic

Table 1. Crystal Data and Experimental Datails for X-Ray Studies

	MTDTPY-$(PF_6)_{0.67}$	MSDTPY-$(AsF_6)_{0.67}$	MSDTPY-$Au(CN)_2$
Formula	$C_{16}H_{12}S_4P_{0.67}F_{4.00}$	$C_{16}H_{12}S_2Se_2As_{0.67}F_{4.00}$	$C_{18}H_{12}N_2S_2Se_2Au_1$
Fw	428.2	552.25	675.31
Cell			
a/Å	8.289(3)	8.373(8)	12.504(2)
b/Å	13.074(4)	13.328(27)	10.342(2)
c/Å	4.302(4)	4.371(4)	7.156(6)
α/°	91.45(5)	91.12(13)	
β/°	103.75(5)	102.81(10)	102.27(3)
γ/°	109.11(12)	148.75(7)	
V/Å^3	447.2(12)	447.2(20)	904.3(7)
Z	1	1	2
D_m g cm^{-3}	1.60	2.02	2.50
D_x g cm^{-3}	1.62	2.05	2.48
Space group	P$\bar{1}$	P$\bar{1}$	P2/c
Crystal shape	Black plate	Black plate	Black block
Crystal dimension	0.50×0.15×0.05 mm	0.50×0.10×0.05 mm	0.30×0.05×0.05 mm
Radiation	graphite-monocromated Mo$K\alpha$ λ=0.7093Å		
μ/cm^{-1}	6.52	61.5	109.0
Abs correction	None	Analytical[a]	None
Scan mode	$2\theta-\omega$		
Scan range	$2\theta \leqq 50°$		
No. of data	1530	1181	1601
No. of data with $F>3\sigma(F)$	1252	877	1318
Decay	less than 1%	less than 1%	less than 3%
No. of variables	143	129	131
R on F_o	0.083	0.116	0.042
R_w on F_o	0.079	0.098	0.039

a) Ref. 8.

Table 2. Final Atomic Coordinates ($\times 10^4$) and Equivalent Isotropic Thermal Parameters, B_{eq} (Å^2) ($\times 10^1$) of MTDTPY-$(PF_6)_{0.67}$.

$^aB_{eq}=8/3\pi^2\sum_i\sum_j U_{ij}a_i^*a_j^*a_ia_j$

Atom	x	y	z	B_{eq}
P	0	0	5000	127(3)
F(1)	0497(16)	−1004(7)	5177(36)	167(6)
F(2)	−1528(15)	−0464(7)	6517(47)	172(7)
F(3)	1517(22)	0506(16)	7687(49)	220(10)
S(1)	1829(1)	5354(1)	8263(3)	33(1)
S(2)	2353(2)	7370(1)	11573(3)	44(1)
C(1)	3323(5)	6642(3)	9622(9)	31(1)
C(2)	4959(5)	6999(4)	9136(10)	30(1)
C(3)	5630(5)	6364(3)	7333(9)	27(1)
C(4)	4640(5)	5294(3)	5903(9)	25(1)
C(5)	2904(5)	4757(3)	6192(8)	25(1)
C(6)	1951(5)	3706(4)	4768(10)	31(1)
C(7)	7327(5)	6847(4)	6949(11)	31(1)
C(8)	3979(10)	8669(6)	12560(21)	64(2)

Table 3. Final Atomic Coordinates ($\times 10^4$) and Equivalent Isotropic Thermal Parameters, B_{eq} (Å^2) ($\times 10^1$) of MSDTPY-$(AsF_6)_{0.67}$.

$^aB_{eq}=8/3\pi^2\sum_i\sum_j U_{ij}a_i^*a_j^*a_ia_j$

Atom	x	y	z	B_{eq}
As	0	0	0	258(15)
F(1)	0593(212)	0279(173)	4595(937)	316(105)
F(2)	−1744(34)	−0547(21)	1749(278)	279(42)
F(3)	0325(49)	−1035(21)	−0385(164)	292(33)
Se	2277(3)	7409(2)	6553(7)	55(1)
S	1842(7)	5338(5)	3243(14)	44(2)
C(1)	3313(28)	6602(17)	4511(45)	39(8)
C(2)	5025(22)	7047(16)	4124(45)	35(7)
C(3)	5637(23)	6374(16)	2323(45)	29(7)
C(4)	4645(25)	5290(16)	0921(43)	27(7)
C(5)	2878(23)	4733(18)	1161(43)	31(7)
C(6)	1960(25)	3674(18)	−0136(51)	37(8)
C(7)	7360(24)	6887(17)	1972(51)	40(8)
C(8)	4090(33)	8826(19)	7212(67)	78(11)

Table 4. Final Atomic Coordinates ($\times 10^4$) and Equivalent Isotropic Thermal Parameters, B_{eq} (Å^2) ($\times 10^1$) of MSDTPY-$Au(CN)_2$.

$^aB_{eq}=8/3\pi^2\sum_i\sum_j U_{ij}a_i^*a_j^*a_ia_j$

Atom	x	y	z	B_{eq}
Au	0	0	5000	43(1)
Se	2799(1)	5442(1)	2452(1)	30(1)
S	4769(2)	6711(2)	4843(3)	25(1)
N	1142(7)	−2714(10)	5770(15)	54(3)
C(1)	3461(6)	7005(7)	3460(11)	22(2)
C(2)	3048(7)	8201(8)	3142(12)	23(2)
C(3)	3613(6)	9373(7)	3755(11)	21(2)
C(4)	4730(5)	9406(7)	4768(11)	19(2)
C(5)	5323(6)	8241(7)	5325(11)	22(2)
C(6)	6431(6)	8290(8)	6286(12)	24(2)
C(7)	3059(7)	10551(8)	3286(13)	26(2)
C(8)	1370(7)	6073(11)	1173(18)	42(3)
C(9)	690(8)	−1727(12)	5441(16)	46(3)

temperature factors have been deposited as Document No. 8927 at the Office of Editor of Bull. Chem. Soc. Jpn.

Reflection Spectra: Reflection spectra were measured within the 200—20000, 700—20000, and 4000—20000 cm^{-1} range for MTDTPY-$(PF_6)_{0.67}$, MSDTPY-$(AsF_6)_{0.67}$ and MTDTPY-$Au(CN)_2$, respectively. The far-infrared region, 200—800 cm^{-1}, was covered with a Fourier-interferrometer equipped with a Ge bolometer. For the mid-infrared region, 700—5000 cm^{-1},another Fourier spectrometer with a HgCdTe detector was used. For the near-infrared and visible regions, a microspectrophotometer was used, which comprised a Carl-Zeiss double monochromator with a PbS cell and a photomultiplier tube (HTV 928). An aluminum mirror and a SiC were used as references in the infrared and visible regions, respectively.

Kramers-Kronig Analysis: The optical conductivity spectra ($\sigma(\omega)$) along the stack axis were obtained by means of Kramers-Kronig transformation. In order to determine the phase shift ($\theta(\omega)$) upon reflection at both ends of measurement, we extrapolated the reflectance with a Drude-like function ($R(\omega)=A-B\omega^{1/2}$) at low frequency and with an inverse fourth-power function ($R(\omega)=C/\omega^4$) at high frequency. A, B, and C were determined with a least-square method within low- and high- frequency regions.

Results and Discussion

Crystal Structure. A: MTDTPY-$(PF_6)_{0.67}$: The bond distances and angles of the MTDTPY molecule are

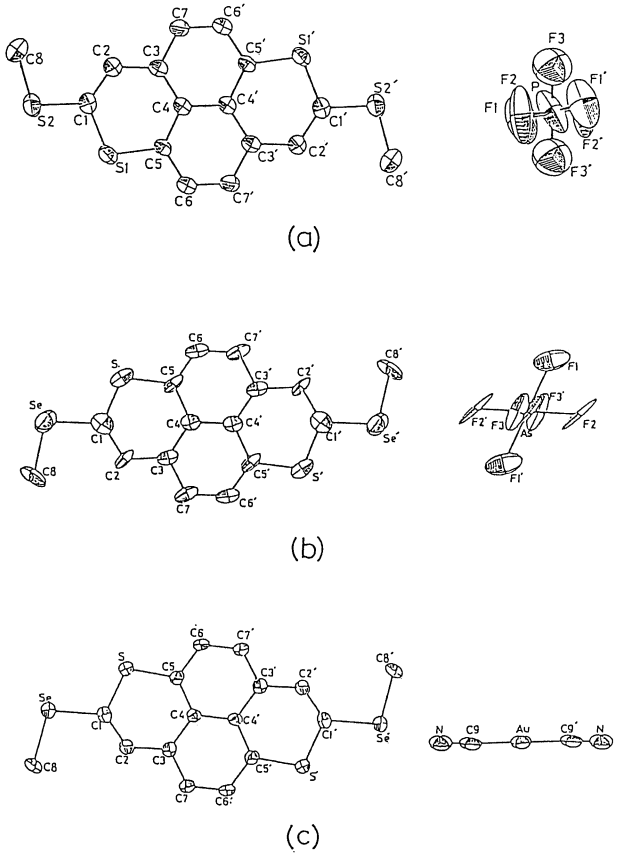

Fig. 2. Molecular structures and it's numbering schemes of (a) MTDTPY-$(PF_6)_{0.67}$: (b) MSDTPY-$(AsF_6)_{0.67}$; (c) MSDTPY-$Au(CN)_2$.

Table 5. Intramolecular Distances (/Å) and Angles (/°) for MTDTP-$(PF_6)_{0.67}$[a)]

	Distances		
S(1)-C(1)	1.732(2)	C(4)-C(5)	1.425(5)
S(1)-C(5)	1.726(5)	C(4)-C(4′)	1.425(5)
S(2)-C(1)	1.739(5)	C(5)-C(6)	1.388(5)
S(2)-C(8)	1.767(6)	C(6)-C(7′)	1.372(6)
C(1)-C(2)	1.356(6)		
C(2)-C(3)	1.437(5)		
C(3)-C(4)	1.414(5)		
C(3)-C(7)	1.400(6)		
	Angles		
C(1)-S(1)-C(5)	103.8(2)	C(3)-C(4)-C(5)	122.2(4)
C(1)-S(2)-C(8)	102.8(3)	C(3)-C(4)-C(4′)	120.6(4)
S(1)-C(1)-S(2)	108.8(2)	C(5)-C(4)-C(4′)	117.2(4)
S(1)-C(1)-C(2)	124.0(4)	S(1)-C(5)-C(4)	123.2(3)
S(2)-C(1)-C(2)	127.2(3)	S(1)-C(5)-C(6)	115.4(3)
C(1)-C(2)-C(3)	123.8(4)	C(4)-C(5)-C(6)	121.4(4)
C(2)-C(3)-C(4)	122.9(4)	C(5)-C(6)-C(7′)	120.4(4)
C(2)-C(3)-C(7)	117.7(4)	C(3)-C(7)-C(6′)	121.0(4)
C(4)-C(3)-C(7)	119.4(4)		

a) Estimated standard deviations are encloded in parentheses.

listed in Table 5, respectively. An ORTEP[10] perspective drawing of the molecular structure and the numbering are shown in Fig. (2a). The methylthio groups deviate from the planar DTPY skeleton: 0.19 Å for C8.

Diffuse spots were found on the plane normal to the c-axis and the superstructure spacing (c') corresponds to 3/2c. The diffuse planes have been interpreted as the superlattice of PF_6^-. Since $3c=2c'$, the PF_6^- superlattice is commensurate with the MTDTPY lattice. As shown in Fig. 3, PF_6^- is aligned at intervals of 6.45 Å along the c-axls. According to this model, the stoichiometric ratio of MTDTPY and PF_6^- is 1 : 0.67. This value is consistent with the density of the crystal, $\rho_m=1.60$ g cm^{-3} and $\rho_m=1.62$ g cm^{-3} for MTDTPY-$(PF_6)_{0.67}$. The temperature factors of PF_6^- have large values along the c-axis (Fig. 3). This result supports the disorder model of PF_6^-.

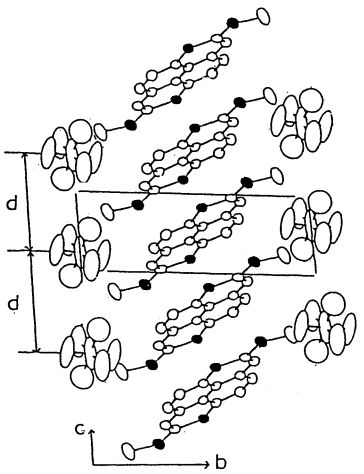

Fig. 3. Anion disorder model of MTDTPY-$(PF_6)_{0.67}$. (d=6.45 Å)

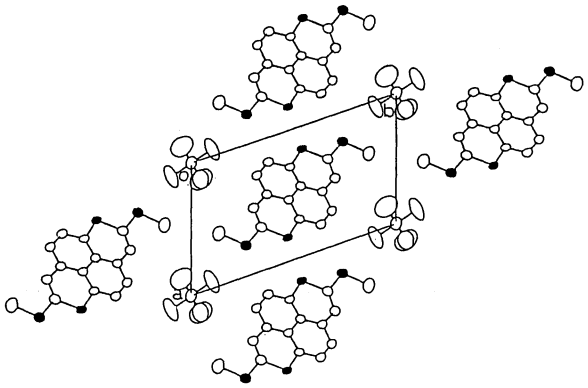

Fig. 4. Crystal structure of MTDTPY-$(PF_6)_{0.67}$ viewed along c-axis.

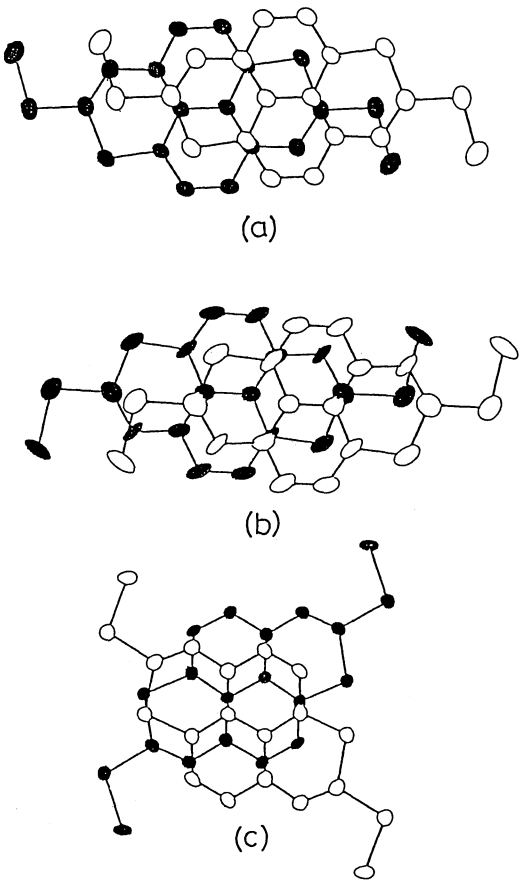

Fig. 5. Overlap mode of MTDTPY and MSDTPY molecules in stack form. (a) MTDTPY-$(PF_6)_{0.67}$ (interplanar distance 3.40 Å); (b) MSDTPY-$(AsF_6)_{0.67}$ (interplanar distance 3.59 Å); (c) MSDTPY-$Au(CN)_2$ (interplanar distance 3.40 Å).

The crystal structure of MTDTPY-$(PF_6)_{0.67}$ is shown in Fig. 4. The stack of MTDTPY is iso-structural with β-MTDTPY-TCNQ complex.[5] The interplanar spacing of MTDTPY along the c-axis is 3.40 Å. The overlap mode of MTDTPY molecules in the stack is shown in Fig. (5a). (This value is shorter than 3.48 Å of the TCNQ complex.) As shown in Fig.

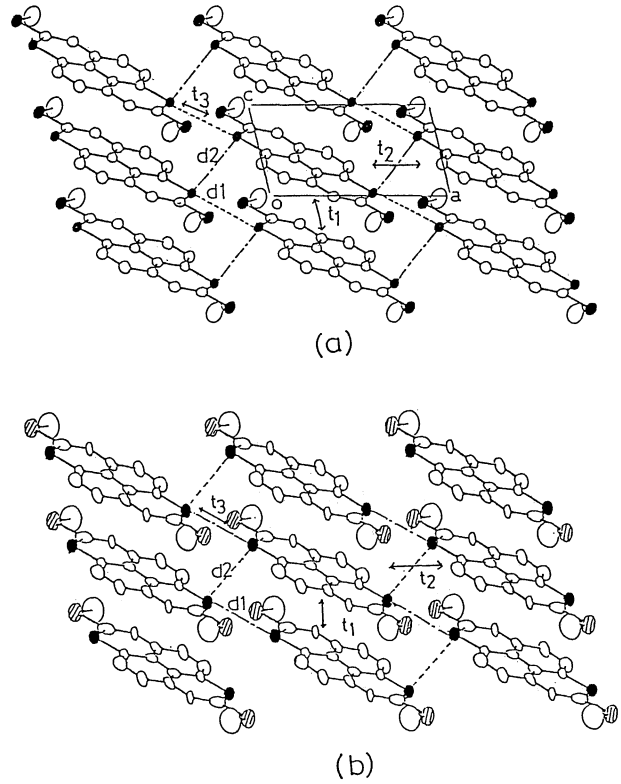

Fig. 6. View of the sheet-like network of MTDTPY and MSDTPY molecules in (a) MTDTPY-$(PF_6)_{0.67}$ (d_1=3.460 Å d_2=3.568 Å); (b) MSDTPY-$(AsF_6)_{0.67}$ (d_1=3.54 Å d_2=3.61 Å).

Table 6. Intramolecular Distances (/Å) and Angles (/°) for MSDTPY-$(AsF_6)_{0.67}$[a]

	Distances		
Se -C(1)	1.90(3)	C(4)-C(5)	1.45(3)
Se -C(8)	1.97(2)	C(4)-C(4′)	1.44(5)
S -C(1)	1.72(2)	C(5)-C(6)	1.40(3)
S -C(5)	1.74(3)	C(6)-C(7′)	1.41(4)
C(1)-C(2)	1.41(3)	As -F(1)	1.96(40)
C(2)-C(3)	1.46(3)	As -F(2)	1.75(8)
C(3)-C(4)	1.45(3)	As -F(3)	1.50(4)
C(3)-C(7)	1.42(3)		
	Angles		
C(1)-Se -C(8)	101(1)	C(3)-C(4)-C(4′)	121(2)
C(1)-S -C(5)	105(1)	C(3)-C(4)-C(5)	123(2)
Se -C(1)-S	110(1)	C(5)-C(4)-C(4′)	116(2)
Se -C(1)-C(2)	122(1)	S -C(5)-C(4)	121(2)
S -C(1)-C(2)	128(2)	S -C(5)-C(6)	117(2)
C(1)-C(2)-C(3)	117(2)	C(4)-C(5)-C(6)	122(2)
C(2)-C(3)-C(4)	126(2)	C(5)-C(6)-C(7′)	122(2)
C(2)-C(3)-C(7)	114(2)	C(3)-C(7)-C(6′)	118(2)
C(4)-C(3)-C(7)	121(2)		

a) Estimated standard deviations are encloded in parentheses.

6(a), there are shorter intercolumnar S-S contacts (3.460(2) Å in the [$\bar{1}$01] direction and 3.568(2) Å in the [100] direction) than the van der Waals contacts. Regarding the intercolumnar contacts, the donor sheets in this crystal are more closely packed than in the case of the TCNQ complex.[5]

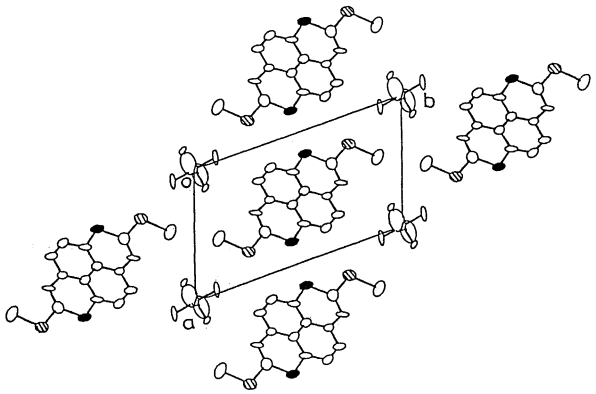

Fig. 7. Crystal structure of MSDTPY-$(AsF_6)_{0.67}$ viewed along c-axis.

B: MSDTPY-$(AsF_6)_{0.67}$: The bond distances and angles of MSDTPY-$(AsF_6)_{0.67}$ are listed in Table 6. An ORTEP perspective drawing of the molecular structure and the numbering are shown in Fig. 2(b). The methylseleno groups deviate from the planar DTPY skeleton: 0.16 Å for C8.

MSDTPY-$(AsF_6)_{0.67}$ is an isostructure of MTDTPY-$(PF_6)_{0.67}$. Similarly to MTDTPY-$(PF_6)_{0.67}$ diffuse spots are found on the plane normal to the c-axis, and the superstructure spacing (c′) corresponds to 3/2c. The diffuse planes are interpreted as being a superlattice of AsF_6^- ions. Since 3c=2c′, the AsF_6^- superlattlce is commensurate with the MSDTPY lattice. The AsF_6^- ions align at intervals of 6.57 Å along the c-axis. According to this model, the stoichiometric ratio of MSDTPY and AsF_6^- is 1:0.67. This is consistent with the result of elemental analysis.

The crystal structure of MSDTPY-$(AsF_6)_{0.67}$ is shown in Fig. 7. MSDTPY molecules are arranged in the same mannar as MTDTPY molecules in MTDTPY-$(PF_6)_{0.67}$. MSDTPY molecules form a stacked column along the c-axis with an interplanar spacing of 3.59 Å. This value is longer than 3.40 Å of MTDTPY-$(PF_6)_{0.67}$. The overlap mode of MSDTPY molecules in the stack is shown in Fig. 5(b). As shown in Fig. 6(b), there are shorter intercolumnar S-S contacts (3.54(2) Å in the [$\bar{1}$01] direction and 3.61(3) Å in the [100] direction) than in the van der Waals contacts.

C: MSDTPY-$Au(CN)_2$: The bond distances and angles of MSDTPY-$Au(CN)_2$ are listed in Table 7. An ORTEP perspective drawing of the molecular structure and the numbering are shown in Fig. 2(c). The methylseleno groups deviate from the planar DTPY skeleton: 0.03 Å for C8. The crystal structure of MSDTPY-$Au(CN)_2$ is shown in Fig. 8. MSDTPY molecules form a stacked column along the c-axis. The overlap mode of MSDTPY molecules in the stacking direction with an interplanar spacing of 3.40 Å and a dihedral angle of 6.6° is shown in Fig. 5(c). The intercolumnar S-S contacts were 3.59 Å and the intercolumnar contacts through substituted

Table 7. Intramolecular Distances (/Å) and Angles (/°) for MSDTPY-Au(CN)$_2$[a)]

	Distances		
Se -C(1)	1.888(7)	C(4)-C(5)	1.426(10)
S -C(8)	1.940(9)	C(3)-C(7)	1.405(11)
S -C(1)	1.749(7)	C(4)-C(4′)	1.408(14)
S -C(5)	1.732(8)	C(5)-C(6′)	1.411(10)
C(1)-C(2)	1.341(11)	C(6)-C(7′)	1.362(11)
C(2)-C(3)	1.425(11)	Au -C(9)	1.979(12)
C(3)-C(4)	1.431(10)	C(9)-N	1.167(16)
	Angles		
C(1)-Se -C(8)	100.2(4)	C(3)-C(4)-C(4′)	120.5(8)
C(1)-Se -C(5)	103.9(4)	C(5)-C(4)-C(4′)	118.5(7)
Se -C(1)-S	110.4(4)	S -C(5)-C(4)	123.6(5)
Se -C(1)-C(2)	127.1(6)	S -C(5)-C(6)	116.1(6)
S -C(1)-C(2)	122.4(6)	C(4)-C(5)-C(6)	120.3(7)
C(1)-C(2)-C(3)	125.8(7)	C(5)-C(6)-C(7′)	120.4(7)
C(2)-C(3)-C(4)	122.9(7)	C(3)-C(7)-C(6′)	121.7(7)
C(2)-C(3)-C(7)	118.5(7)	Au -C(7)-N	176.4(8)
C(4)-C(3)-C(7)	118.6(7)	C(9)-Au -C(9′)	180.0(8)
C(3)-C(4)-C(5)	121.0(7)		

a) Estimated standard deviations are encloded in parentheses.

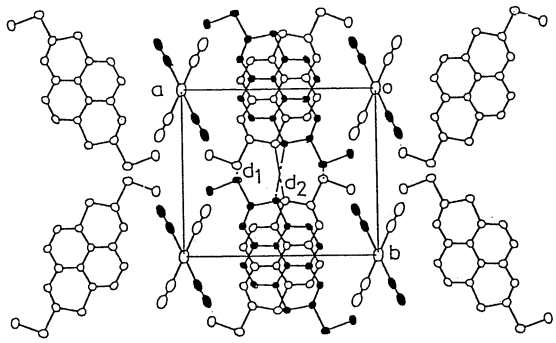

Fig. 8. Crystal structure of MSDTPY-Au(CN)$_2$ viewed along c-axis. (d_1=3.69 Å d_2=3.59 Å).

selenium atoms were 3.69 Å (See Fig. 8).

Estimation of Transfer Integrals. In order to estimate interaction between MTDTPY molecules in MTDTPY-(PF$_6$)$_{0.67}$ and MSDTPY molecules in MSDTPY-(AsF$_6$)$_{0.67}$, we calculated the transfer integrals for some of the directions with the highest occupied orbital by the PPP method. In MTDTPY-(PF$_6$)$_{0.67}$, values of t_1=0.249 eV, t_2=0.005 eV, and t_3=0.004 eV were calculated for directions [001], [100], and [$\bar{1}$01], respectively, in MSDTPY-(AsF$_6$)$_{0.67}$; values of t_1=0.150 eV, t_2=0.004 eV and t_3=0.003 eV were calculated for the directions [001], [100], and [$\bar{1}$01], respectively (See Fig. 6). From the large anisotoropy in MTDTPY-(PF$_6$)$_{0.67}$ and MSDTPY-(AsF$_6$)$_{0.67}$, it is expected that, in spite of short intercolumnar S-S contacts, the MTDTPY and MSDTPY columns formed one-dimensional conducting chains. According to the tight-binding model, the HOMO band is partially filled when the formal charge of a molecule is +0.67. The dc conductivity of a single crystal at ambient temperature along the stack axis is weakly temperature dependent with 43 S cm^{-1} for MTDTPY-(PF$_6$)$_{0.67}$ and 36 S cm^{-1} for MSDTPY-(AsF$_6$)$_{0.67}$. Though these values correspond to that of a moderate organic conductor, they show semiconductlve behavior within the low-temperature region.[11)]

Reflection spcctra. A: MTDTPY-(PF$_6$)$_{0.67}$: The reflection spectra of MTDTPY-(PF$_6$)$_{0.67}$ on [010] are shown in Fig. 9. The reflection spectra of a single crystal showed the typical behavior of a one-dimensional metallic column. The reflectance with light polarized parallel to the c-axis is much higher than that of the perpendicular direction. A Drude-type reflectance edge could be discerned around 6000 cm^{-1} indicating the presence of a free carrier. In the stacking direction, a number of sharp peaks were found in the 500—1500 cm^{-1} infrared region. Strong peaks (836, 902, 1000, 1122, 1330, 1394, 1422 cm^{-1}) were found in the IR spectra of MTDTPY. However, the vibrational peaks in the perpendicular direction are relatively weak and most vibrational peaks of in-plane mode should not be observed in the stacking direction. The A_{1g}-type Raman modes appear in the infrared spectra through a coupling with an out-of-plane electronic transition of the charge-transfer character (electorn-molecular vibration coupling).[12)] Therefore, the positions of these peaks (1190, 1330, 1420 cm^{-1}) may correspond to the Raman spectra of MTDTPY (1215, 1327, 1365, 1445 cm^{-1}). The peak at

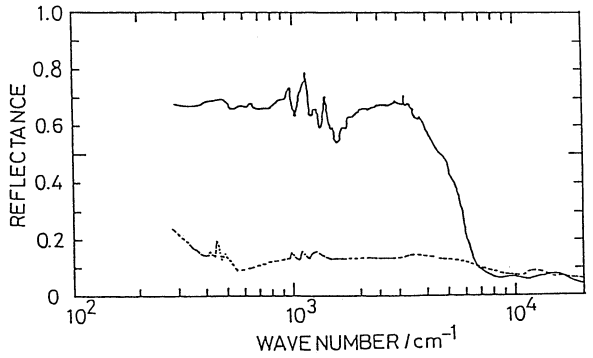

Fig. 9. Reflection spectra on [010] of MTDTPY-(PF$_6$)$_{0.67}$. (solid line: parallel to c-axis, dashed line: perpendiculer to c-axis).

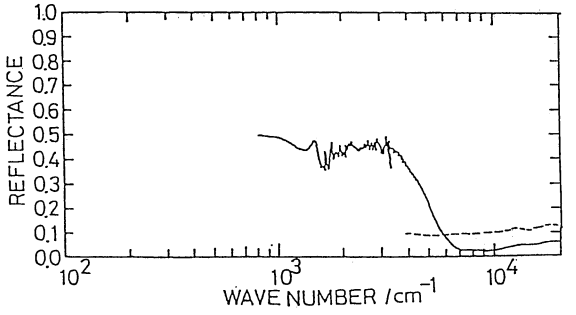

Fig. 10. Reflection spectra on [010] of MSDTPY-(AsF$_6$)$_{0.67}$. (solid line: parallel to c-axis, dashed line: perpendiculer to c-axis).

1000 cm^{-1} may correspond to the IR mode, and the peak at 810 cm^{-1} is due to PF_6^-.

B: MSDTPY-$(AsF_6)_{0.67}$: The reflection spectra of MSDTPY-$(AsF_6)_{0.67}$ on [010] are shown in Fig. 10. As well as MTDTPY-$(PF_6)_{0.67}$, the reflection spectra of the single crystal showed the typical behavior of a one-dimensional metallic column. The reflectance with light polarized parallel to the c-axis was much higher than that in the perpendicular direction. A Drude-type reflectance edge could be discerned around 6000 cm^{-1}, indicating the presence of a free carrier. Compared with MTDTPY-$(PF_6)_{0.67}$, however, the reflectance is relatively low.

C: MSDTPY-$Au(CN)_2$: Since the stoichiometrlc ratio of MSDTPY and $[Au(CN)_2]^-$ is 1:1, MSDTPY molecules are fully oxidized and exist as $MSDTPY^+$ ions. The reflection spectra of MSDTPY-$Au(CN)_2$ on [100] are shown in Fig. 11. Obviously, a strong electronic transition exists for polarization parallel to the stacking axis; however, no clear transitions could be found for polarization perpendicular to the stack axis. This transition is assigned to the charge-transfer band between MSDTPY radical cations. According to a simple harmonic-oscillator model, the transition energy, oscillator strength and half-band width exist at 6000 cm^{-1}, 0.6 and 2800 cm^{-1}, respectively. Since MSDTPY molecules are fully oxidized, this transition energy corresponds to an on-site Coulmb repulsion (U). This value is relatively small compared to TCNQ,[12] showing that U is smaller for a large layered conjugated system and that MSDTPY is suitable for the component of organic metals. Since the result gives a smaller value of U, the dc conductivity at room temperature[11] is relatively high (σ=0.15 $S\,cm^{-1}$), compared with other fully oxidised charge-transfer complexes.

Optical Properties and One Dimensional Localization Models. The optical conductivity ($\sigma(\omega)$) and the real part of the dielectrlc constant ($\varepsilon'(\omega)$) spectra for MTDTPY-$(PF_6)_{0.67}$ and MSDTPY-$(AsF_6)_{0.67}$ are shown in Figs. 12 and 13, respectively. According to the relatively low dc conductivities (~10 $S\,cm^{-1}$) of these materials, the optical conductivities of the DTPY families have their maxima in the infrared region, and decrease with $\omega \to 0$. The real parts of the dielectric functions showed positive values with the low-frequency region. Such behavior is not described by the simple Drude model.

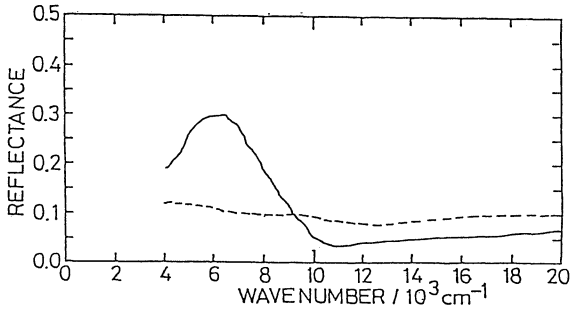

Fig. 11. Reflection spectra on [100] of MSDTPY-$Au(CN)_2$. (solid line: parallel to c-axis, dashed line: perpendiculer to c-axis).

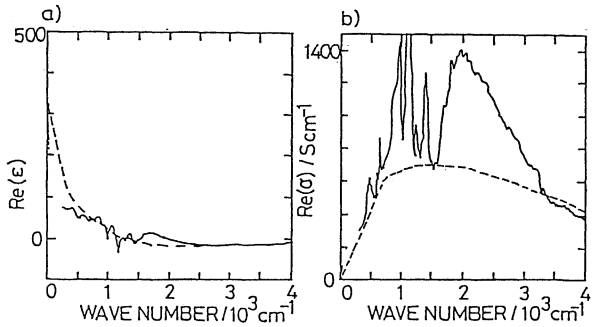

Fig. 12. Frequency dependence of a) $Re(\varepsilon)$ and b) σ for MTDTPY-$(PF_6)_{0.67}$. The solid line repersents experiment and the dash line represents theory at τ_i^{-1}=2400 cm^{-1}, ω_p^{-1}=14000 cm^{-1}, and ε_{core}=3.0.

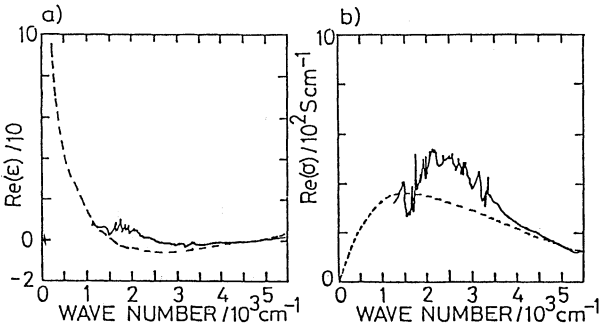

Fig. 13. Frequency dependence of a) $Re(\varepsilon)$ and b) σ for MSDTPY-$(AsF_6)_{0.67}$. The solid line repersents experiment and the dash line represents theory at τ_i^{-1}=2400 cm^{-1}, ω_p=10000 cm^{-1}, and ε_{core}=3.5.

We have pointed out that a one-dimensional localization model is useful for describing the electronic structre of MTDTPY complexes.[14] Mott et al.[15] suggested that the optical conductivity ($\sigma(\omega)$) in a one-dimensional metal disordered by impurities or lattice defects has the form $\omega^2(\ln\omega)^2$ in the $\omega\tau_i \ll 1$ region.

Berezinsky[16] showed that backward scattering is dominant in one-dimensional disordered metals, and derived a formula which is valid for any $\omega\tau_i$, where τ_i is the mean lifetime with respect to scattering on a disordered potential. Gogolin[17,18] solved the Berezinsky formula using numerical methods.

At the limit $\omega\tau_i \gg 1$, this model shows $\sigma(\omega)$ and $\varepsilon(\omega)$ of the Drude type: $\sigma(\omega) \sim 2\sigma_0/(\omega\tau_i)^2$, $\varepsilon(\omega) \sim -\varepsilon_0/(\omega\tau_i)^2$. At the limit $\omega\tau_i \ll 1$, this model shows Mott's form: $\omega^2(\ln\omega)^2$.

A one-dimensional MTDTPY and MSDTPY chain may be described by a model involving a random potential created by impurities, lattice defects and a disorder of PF_6^- and AsF_6^-. With Gogolin's method for numerical calculations, the optical conductivity ($\sigma(\omega)$) and dielectric constant ($\varepsilon(\omega)$) of MTDTPY-

$(PF_6)_{0.67}$ and MSDTPY-$(AsF_6)_{0.67}$ were simulated as the dashed lines shown in Figs. 12 and 13, respectively. The fitting parameters are shown in Table 8. Here, ω_p is the plasma frequency.

According to the tight-binding model, the effective mass (m^*) is estimated from ω_p follows:

$$m^* = \frac{N e^2}{\pi c^2 \omega_p^2}. \quad (1)$$

Here, c is the velocity of light and N is the density of carriers. The transfer integral (t) in a stacked column is expressed by

$$t = \frac{\rho^2 \pi \hbar^2}{4 m^* d^2 \sin(\rho \pi/2)}, \quad (2)$$

where d is the cell constant of the stack axis and ρ is a number of carriers per site. The estimated values of t from Eq. 2 are shown in Table 8.

The smaller value of ω_p=10000 cm^{-1} in MSDTPY-$(AsF_6)_{0.67}$ than that of ω_p=14000 cm^{-1} in MTDTPY-$(PF_6)_{0.67}$ correspond to a larger value of m^*. Therefore, the transfer integral (t) in MSDTPY-$(AsF_6)_{0.67}$ is smaller than that in MTDTPY-$(PF_6)_{0.67}$. This result is consistent with a large interplanar spacing in the stacking axis. The values of t estimated from the optical spectra were in good agreement with that estimated by a molecular orbital calculation. (See Table 8)

In MTDTPY-$(PF_6)_{0.67}$ and MSDTPY-$(AsF_6)_{0.67}$ this model can not completely explain the dominant strong peak in the infrared region. Nevertheless, the theoretical curve of an electron localization model for the background contribution agrees with the experimental data.

The mean free path of a localized system is given by $l_i = v_F \tau_i$. The values of v_F were estimated using

$$v_F = \frac{\rho^2 \pi \hbar}{2\sqrt{2} m^* d \sin(\rho \pi/2)}. \quad (3)$$

The localization length ($l_{loc}=4l_i$[17]) was estimated to be 19.2 and 11.0 Å for MTDTPY-$(PF_6)_{0.67}$ and MSDTPY-$(AsF_6)_{0.67}$, respectively.

Since the Berezinsky equation is valid for a weak random potential, it may not be suitable for a relatively strongly disordered case created by PF_6^- and AsF_6^- ions. Gogolin applied the Berezinsky diagram technique to the case of a strong random potentlal.[17] However, the behavior of one-dimensional carriers in a strong random potential has not yet been clarified.

The large value of the scatterlng rate (τ_i^{-1}~2400 cm^{-1}) in MTDTPY-$(PF_6)_{0.67}$ and MSDTPY-$(AsF_6)_{0.67}$ indicates that the localized electron model is more appropriate for describing the electronic structure.

In a one-dimensional localization model, the conduction mechanism is mainly hopping electrons. A moderate metallic conductiviy at room temperature may be contradictory to such an localized electron model. However, Kaveh et al.[19] suggested that intramolecular phonons have a delocalizing effect on the electrons and that the resistance is mainly due to scattering by a disordered potential. Since the reflection spectra of MTDTPY-$(PF_6)_{0.67}$ show a strong electron-molecular vibration coupling, σ may have weak temperature dependence due to disordred potentials.

Table 8. Fitting Parameters of Localization Model

	MTDTPY-$(PF_6)_{0.67}$	MSDTPY-$(AsF_6)_{0.67}$
ω_p/cm^{-1}	14000	10000
τ_i^{-1}/cm^{-1}	2400	2400
ε_{core}	3.0	3.5
t/eV (opt)	0.233	0.120
t/eV (calcd)	0.249	0.150

Conclusion

MTDTPY-$(PF_6)_{0.67}$ and MSDTPY-$(AsF_6)_{0.67}$ crystals have superstructures of PF_6^- or AsF_6^-. MTDTPY molecules in MTDTPY-$(PF_6)_{0.67}$ and MSDTPY molecules in MSDTPY-$(AsF_6)_{0.67}$ form one-dimensional conducting columns parallel to the c-axis. In order to explain electronic structures of these salts, we assume a one-dimensional disordered model; electrons in MTDTPY or MSDTPY columns are relatively strongly scattered and are localized due to the disordered potential of PF_6^- or AsF_6^- ions. Values of τ_i^{-1}= 2400 cm^{-1} (τ_i=2.2×10^{-15} s) and ω_p=14000 cm^{-1} in MTDTPY-$(PF_6)_{0.67}$ and values of τ_i^{-1}=2400 cm^{-1} (τ_i=2.2×10^{-15} s) and ω_p=10000 cm^{-1} in MSDTPY-$(AsF_6)_{0.67}$ were obtained for free carriers in the column.

The MSDTPY-$Au(CN)_2$ crystal is a fully oxdized radical salt and MSDTPY molecules form segregated stacks along the c-axis. From the reflection spectra, the on-site Coulomb repulsion U was estimated as 6000 cm^{-1} (0.75 eV). This relatively small value of U indicates that MSDTPY is suitable for the component of organic metals.

References

1) For general reviews, see: F. Wudl, *Acc. Chem. Res.*, **17**, 227 (1984).

2) D. Jerome, A. Mazaud, M. Dibault, K. Bechgaard, *J. Phys. Lett. (Paris)*, **41**, 95 (1980).

3) E. B. Yagubskii, I. F. Shchegolev, V. N. Lauhin, P. A. Kononovich, M. V. Kartsovnik, A. V. Zvarykina, and L. I. Buravov, *JETP Lett.*, **39**, 12 (1984).

4) K. Nakasuji, H. Kubota, T. Kotani, I. Murata, G. Saito, T. Enoki, K. Imaeda, H. Inokuchi, M. Honda, C. Katayama, and J. Tanaka, *J. Am. Chem. Soc.*, **108**, 3460 (1986).

5) K. Nakasuji, M. Sasaki, T. Kotani, I. Murata, T. Enoki, K. Imaeda, H. Inokuchi, A. Kawamoto, and J. Tanaka, *J. Am. Chem. Soc.*, **109**, 6970 (1987).

6) A. Furusaki, *Acta Cryst.*, **A35**, 220 (1979).

7) P. Main, S. Huli, L. Lessinger, G. Germain, J. P. Declercq, and M. M. Woolfson, MULTAN78, "A System of Computer Programs for the Automatic Solution of Crystal Structures from X-ray Diffraction Data," Univ. of York,

England and Louvain, Belgium (1978).
8) C. Katayama and M. Honda, *CRYSTAN*, The Computer Center of Nagoya University Library Program.
9) *International Tables for X-ray Crystallography* (1974). Kynoch Press, Birmingham: Vol IV, pp. 71—151.
10) C. K. Johnson, ORTEP, Report ORNL-3794, Oak Ridge National Laboratory, Tennessee (1965).
11) T. Imaeda, Private communication.
12) M. J. Rice, *Phys. Rev. Lett.*,**37**, 36 (1976).
13) J. Tanaka, M. Tanaka, T. Kawai, T. Takabe, and O. Maki, *Bull. Chem. Soc. Jpn.*, **9**, 2358 (1976).
14) A. Kawamoto, J. Tanaka, M. Sasaki, I. Murata, and K. Nakasuji, *Bull. Chem. Soc. Jpn.*, **63**, 2146 (1990).
15) N. F. Mott, *Philos. Mag.*, **17**, 1259 (1968).
16) V. L. Brerezinsky, *Sov, Phys. JETP*, **38**, 620 (1974).
17) A. A. Gogolin, *Phys. Rep.*, **86**, 1 (1982).
18) A. A. Gogolin and V. I. Mel'nikov, *Phys. Status Solidi B*, **88**, 377 (1978).
19) M. Kaveh, M. Weger, and H. Gutfreund, *Solid State Commun.*, **31**, 83 (1979).